



**Providing Choice & Value**

Generic CT and MRI Contrast Agents



CONTACT REP

**AJNR**

This information is current as  
of July 23, 2025.

## **Doppler Ultrasound Flow Reversal in the Superior Sagittal Sinus to Detect Cerebral Venous Congestion in Vein of Galen Malformation**

S. Schwarz, F. Brevis Nuñez, N.R. Dürr, F. Brassel, M. Schlunz-Hendann, A. Feldkamp, T. Rosenbaum, U. Felderhoff-Müser, K. Schulz, C. Dohna-Schwake and N. Bruns

*AJNR Am J Neuroradiol* 2023, 44 (6) 707-715

doi: <https://doi.org/10.3174/ajnr.A7891>

<http://www.ajnr.org/content/44/6/707>

# Doppler Ultrasound Flow Reversal in the Superior Sagittal Sinus to Detect Cerebral Venous Congestion in Vein of Galen Malformation

 S. Schwarz,  F. Brevis Nuñez,  N.R. Dürr,  F. Brassel,  M. Schlunz-Hendann,  A. Feldkamp,  T. Rosenbaum, U. Felderhoff-Müser,  K. Schulz,  C. Dohna-Schwake, and  N. Bruns



## ABSTRACT

**BACKGROUND AND PURPOSE:** Vein of Galen malformation is a rare congenital cerebrovascular malformation. In affected patients, increased cerebral venous pressure constitutes an important etiologic factor for the development of brain parenchymal damage. The aim of this study was to investigate the potential of serial cerebral venous Doppler measurements to detect and monitor increased cerebral venous pressure.

**MATERIALS AND METHODS:** This was a retrospective monocentric analysis of ultrasound examinations within the first 9 months of life in patients with vein of Galen malformation admitted at <28 days of life. Categorization of perfusion waveforms in the superficial cerebral sinus and veins into 6 patterns was based on antero- and retrograde flow components. We performed an analysis of flow profiles across time and correlation with disease severity, clinical interventions, and congestion damage on cerebral MR imaging.

**RESULTS:** The study included 44 Doppler ultrasound examinations of the superior sagittal sinus and 36 examinations of the cortical veins from 7 patients. Doppler flow profiles before interventional therapy correlated with disease severity determined by the Bicêtre Neonatal Evaluation Score (Spearman  $\rho = -0.97$ ,  $P < .001$ ). At this time, 4 of 7 patients (57.1%) showed a retrograde flow component in the superior sagittal sinus, whereas after embolization, none of the 6 treated patients presented with a retrograde flow component. Only patients with a high retrograde flow component (equal or more than one-third retrograde flow,  $n = 2$ ) showed severe venous congestion damage on cerebral MR imaging.

**CONCLUSIONS:** Flow profiles in the superficial cerebral sinus and veins appear to be a useful tool to noninvasively detect and monitor cerebral venous congestion in vein of Galen malformation.

**ABBREVIATIONS:** AV = arteriovenous; BNES = Bicêtre Neonatal Evaluation Score; cMRI = cerebral MR imaging; FP = flow profile; MPV = median prosencephalic vein of Markowski; SSS = superior sagittal sinus; US = ultrasound; VGAM = Vein of Galen (aneurysmal) malformation

**V**ein of Galen (aneurysmal) malformation (VGAM) is a rare, complex, congenital cerebrovascular malformation. Arteriovenous (AV) fistulas or malformations between the persistent median prosencephalic vein of Markowski (MPV) and various arterial


feeding vessels or both result in intracerebral shunts between the arterial and venous systems.<sup>1</sup> This arteriovenous connection causes a loss of cerebral arterial resistance with redistribution of blood to the detriment of the brain and other organ systems, sometimes culminating in high-output cardiac failure. Despite modern therapeutic interdisciplinary interventions, the mortality in neonatal manifestation is approximately 40%, and 50% of survivors have poor neurodevelopmental outcomes.<sup>2-4</sup>

Besides reduced arterial cerebral organ perfusion, increased cerebral venous pressure plays a key role in the development of progressive parenchymal brain damage. Arterialization of the MPV and the cerebral sinus causes a massive increase in cerebral venous pressure, with subsequent functional outflow obstruction, leading to congestion, venous ischemia, and hydrocephalus mal-resorptivus.<sup>5-8</sup> Cerebral venous hypertension can be exacerbated by high venous return due to excessive shunt volumes with cardiac volume overload and backward failure of the right heart.<sup>9</sup>

Received February 14, 2023; accepted after revision May 3.

From the Clinic for Pediatrics and Adolescent Medicine (S.S., F.B.N., A.F., T.R.), Clinic for Radiology and Neuroradiology (N.R.D., F.B., M.S.-H., K.S.), and Center for Pediatric Interventional Radiology/Neuroradiology and Interventional Treatment of Vascular Malformations (F.B.), Sana Clinics Duisburg, Duisburg, Germany; and Clinic for Pediatrics I (U.F.-M., C.D.-S., N.B.) and Centre for Translational Neuro- and Behavioural Sciences (U.F.-M., C.D.-S., N.B.), University Hospital Essen, University of Duisburg-Essen, Essen, Germany.

Please address correspondence to Simone Schwarz, MD, Clinic for Pediatrics and Adolescent Medicine, Neonatal and Pediatric Intensive Care Unit, Sana Clinics Duisburg, Zu den Rehwiesen 9-11, 47055 Duisburg, Germany; e-mail: simone.schwarz@sana.de

 Indicates open access to non-subscribers at [www.ajnr.org](http://www.ajnr.org)

 Indicates article with online supplemental data.

<http://dx.doi.org/10.3174/ajnr.A7891>

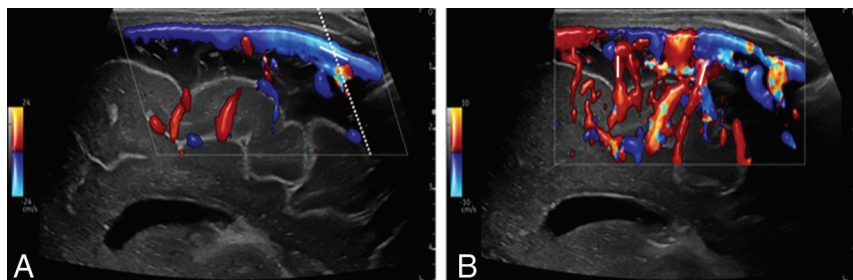


**FIG 1.** Doppler imaging protocol of the SSS and cortical veins in a median sagittal section. A, SSS in median sagittal section in color-coded Doppler US with tilted Doppler beam (dotted line) and corresponding angular correction (white line). B, Cortical arteries and veins in sagittal section in color-coded Doppler US show possible measurement points (white lines).

Furthermore, a maturation disorder of the sinu-jugular connection due to flow stress in the vessel wall may lead to bilateral stenosis of the jugular bulb, further increasing cerebral venous pressure.<sup>10–12</sup> Thus, venous congestion may persist even after marked reduction of the shunt volume.

Cerebral venous congestion leads mainly to white matter injury and subependymal atrophy, making it one of the main factors for progressive brain damage in VGAM.<sup>3,10</sup> To date, there is no tool for early noninvasive detection and serial assessment of cerebral venous congestion. Currently, the best method is cerebral MR imaging (cMRI), which only shows indirect signs and direct parenchymal damage due to chronic venous congestion, such as congested veins, congestive edema, microhemorrhages, calcifications, and atrophy.<sup>13–15</sup>

The aim of this study was to investigate the potential of serial venous ultrasound (US) Doppler measurements to detect and monitor increased cerebral venous pressure in VGAM.

## MATERIALS AND METHODS

This retrospective, monocentric study included all neonates with VGAM younger than 28 days admitted to the tertiary care neonatal intensive care unit at the Sana Hospital Duisburg between January and June 2022. All examinations were performed by a board-certified neonatologist with >10 years of experience in cerebral US and Doppler US (S.S.) according to a standardized local protocol.

Eligible patients were identified via the electronic patient administration system, and clinical data were collected from the digital patient management systems including the PACS. The Bicêtre Neonatal Evaluation Score (BNES), a validated clinical score with therapeutic and prognostic significance, was recorded before the first cMRI to assess disease severity (Online Supplemental Data).<sup>16,17</sup>

Approval of the study was granted by the Ethics Committee of the Medical Faculty of the University Hospital Essen (22–10801-BO).

### US Protocol

To assess the time course of US Doppler flow profiles (FPs), we analyzed the examination before the first cMRI (T1), after the first cMRI/embolization (T2), after 5–7 days (T3), and before discharge (T4) of each patient during the first inpatient stay. After discharge, the available examinations were evaluated on an individual basis.

All US scans were obtained using 1 of 2 high-end US machines (LOGIQ S8/ LOGIQ E10s R3; GE Healthcare) equipped with high-resolution linear transducers (ML5-15-D or ML4-20-D; GE Healthcare). Venous cerebral US Doppler flow measurements were documented only in calm, preferably sleeping, infants. US Doppler FPs in the superior sagittal sinus (SSS) were recorded using a median sagittal section (Fig 1). First, the SSS was visualized in a longitudinal section at a low penetration depth in B-mode and color-coded Doppler US with flow displayed over the entire vessel

section. Next, an angle-corrected pulsed Doppler time-frequency analysis of intravascular flow in a far posterior vessel segment before the junction of any VGAM drainage veins was performed. The sample volume was adapted until the entire width of the vessel was captured. Visual and acoustic reassurance of an optimal time-frequency Doppler signal ensured that the sample volume passed through the center of the vessel. Doppler FPs in the cortical veins were measured with the same transducer, following the same optimization steps (Fig 2B). The FPs were only evaluated for this study if the Doppler flow curves had sufficient image quality, ie, correct positioning of the sample volume, correct wall filter, correct pulse repetition frequency, and sufficient Doppler signal for at least 5 seconds.

### Classification of US Doppler FPs

Following Ikeda et al,<sup>18</sup> the FPs were classified into 6 different types (Fig 2): FP1: low alterations of the flow amplitude, minimum velocity never less than half of the maximum velocity; FP2: increased undulation, minimum speed less than half of the maximum speed; FP3: increased undulation, minimum speed dropping to 0 cm/s or retrograde flow; FP4: retrograde flow component with pulsatile retrograde flow; FP5: high retrograde flow, equal or more than one-third retrograde flow of the total Doppler flow; and FP6: complete retrograde flow.

### MR Imaging

Timing of endovascular therapy was determined by interdisciplinary consensus based on clinical and sonographic findings. The first cMRI was performed with the patient under the same anesthesia as in the first procedure. Assessment of the first cMRI and the follow-up cMRI after 1–10 months was retrospectively performed by an experienced neuroradiologist (N.R.D.), blinded to the clinical course using a structured report and a previously described scoring system for structural brain abnormalities.<sup>19</sup> Damage to the brain parenchyma was classified as no lesion, mild lesion, moderate lesion, and severe lesion. All structural abnormalities were documented, especially signs of brain atrophy, medullary lesions, ischemic or hemorrhagic infarcts or their remnants, hemorrhages, and damage due to venous congestion.

### Endovascular Therapy

In most centers, endovascular therapy of a VGAM is performed via a transarterial approach with exclusive embolization of the arterial feeders apart from the point of shunting. According to our clinical routine, combined therapy with arterial and venous

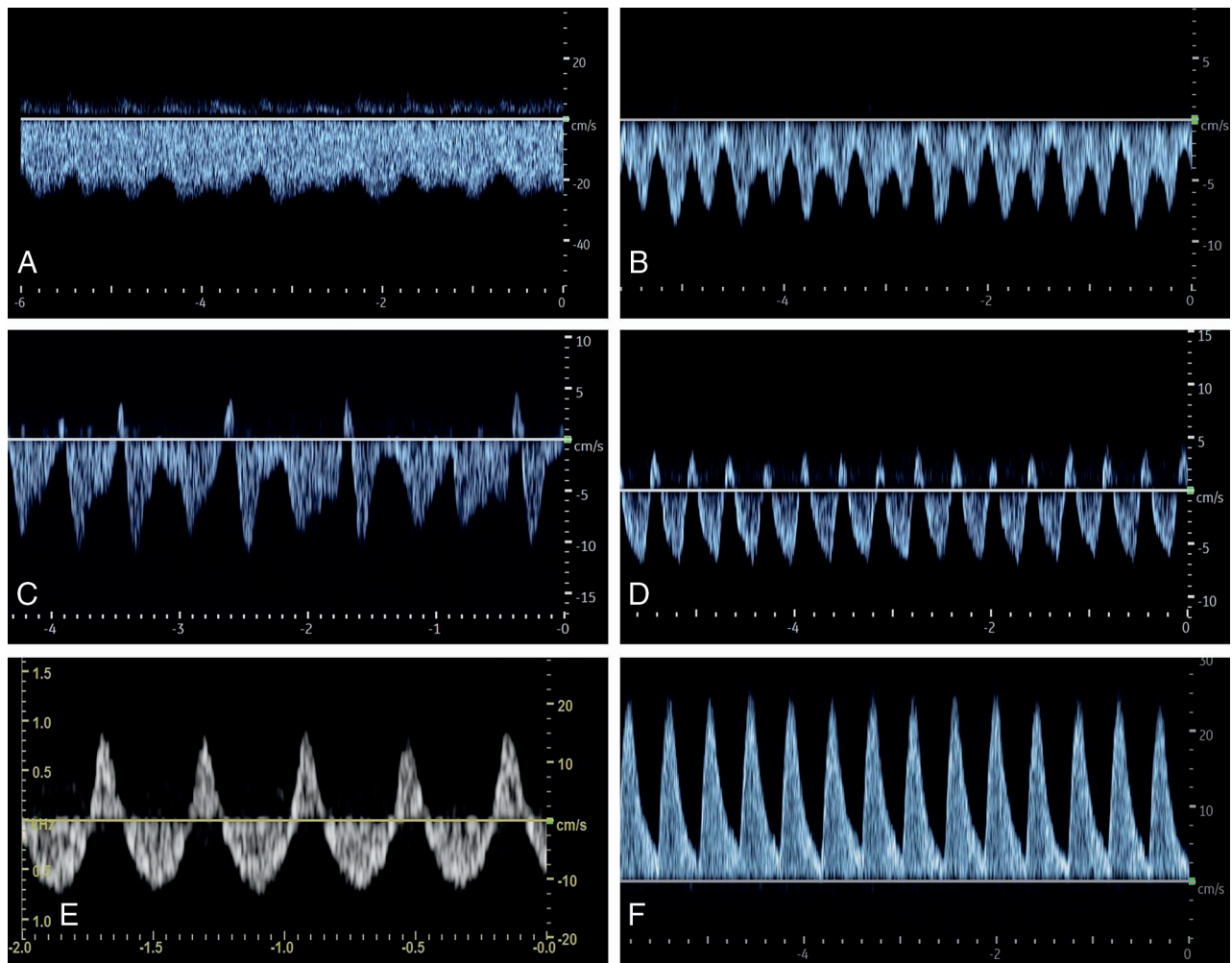


**FIG 2.** Classification of Doppler FPs of the SSS in neonates with vein of Galen malformation. A, FP1: Doppler FP with low fluctuation, minimum velocity, never less than half of the maximum velocity. B, FP2: Increased fluctuations of the flow velocities with minimum velocity less than half of the maximum velocity. C, FP3: Doppler FP with intermittent retrograde flow. D, FP4: Doppler FP with pulsatile retrograde flow. E, FP5: Doppler FP with a high retrograde flow (equal or more than one-third retrograde flow of the total Doppler flow). F, FP6: Doppler FP with complete retrograde flow.

access was performed for precise occlusion of AVFs, with high flow exactly at the shunting point with coils and/or ethylene-vinyl alcohol. To obtain direct access to the inflowing artery at the entry point of the dilated persistent MPV, we introduced superselective arterial feeder probing in combination with retrograde transvenous access using the “looping technique” or “kissing microcatheter technique.”<sup>20</sup>

### Statistical Analyses

Categoric variables are summarized as counts and relative frequencies; continuous variables are presented as median and range. The Spearman  $\rho$  was calculated to assess the association of FPs in the SSS and BNES. SAS Enterprise Guide 8.3 (SAS Institute) was used to perform statistical analyses.

## RESULTS

A total of 7 neonates with VGAM with a median gestational age of 38 1/7 (range, 34 2/7–41 6/7) and a median birth weight of 3380 g (range, 2220–4250 g) were admitted in the study period (Fig 3 and Online Supplemental Data). They were admitted as

inpatients at a median age of 2 days (range, 1–13 days) with a median BNES of 18 (range, 7–21). According to Lasjaunias,<sup>16</sup> 3 of 7 (42.9%) of the AV malformations were choroidal, 3 of 7 (42.9%) were mural, and 1 of 7 (14.3%) was a mixed type.<sup>17</sup>

One patient was treated palliatively due to severe brain parenchymal damage at the initial presentation and died in the second week of life. All other patients underwent endovascular therapy at a median of 4.5 days (range, 1–14 days) after birth in the Department of Interventional Neuroradiology and were discharged alive. One neonate experienced intraventricular hemorrhage and posthemorrhagic hydrocephalus after the intervention. No other neonates developed complications from the procedure (Online Supplemental Data).

### US Doppler Flow Measurements during Initial Therapy

All 7 patients underwent a standardized US before and 1 day after the first embolization and after cMRI in the palliative case (T1 + T2). All survivors were examined before discharge (T4), and 5 of the 6 survivors underwent an additional examination 5–7 days after embolization (T3). Thus, 26 Doppler US examinations of



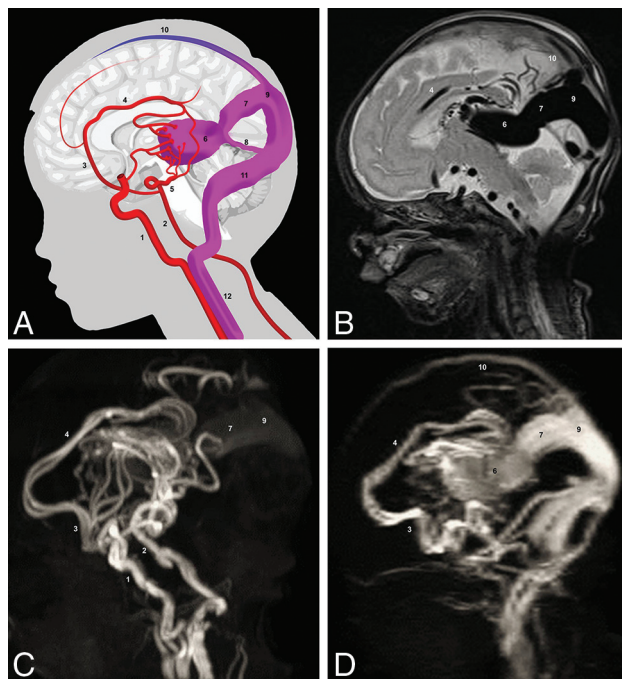


**FIG 3.** Scheme and MR imaging of a VGAM. A, Simplified scheme of VGAM. B, Sagittal T2-weighted MR image. C, Arterial TOF-MRA. D, Venous TOF-MRA. 1) internal carotid artery; 2) basilar artery; 3) anterior cerebral artery; 4) pericallosal artery; 5) posterior cerebral artery; 6) dilated MPV; 7) falcine sinus; 8) straight sinus; 9) accessory confluence; 10) SSS; 11) transverse sinus; 12) internal jugular vein.

the SSS and 25 examinations of the cortical veins were included in this analysis (Fig 4A).

Overall, 4 of 7 (57.1%) of the Doppler flow measurements at T1 showed a retrograde flow component in the SSS. After embolization, no patient had a retrograde flow component. One week after the first embolization, patient 5 developed an increasing retrograde flow component that progressed to complete retrograde flow in the SSS and cortical veins until discharge.

At all time points, correlating abnormal FPs in the cortical veins were observed only when the SSS had a high retrograde flow component (FP5 + 6) (Online Supplemental Data).

Before interventional therapy, US Doppler FPs correlated with disease severity determined by BNES ( $\rho = -0.97$ ; 95% CI,  $-0.995$  to  $-0.787$ ;  $P < .0001$ ). Pathologic FPs occurred more frequently with low BNESs (Fig 4B).

#### Correlation to Congestion Damage on cMRI

Only 2 patients showed severe venous congestion damage on cMRI (Online Supplemental Data). Patient 1 showed severe cerebral damage on the first cMRI. Patient 5 showed cerebral injury with moderate atrophy, white matter damage, and hydrocephalus ex-vacuo and malresorptivus due to venous congestion on the second MR imaging. Both patients had high or complete retrograde flow in the SSS and cortical veins before cMRI. No other patient showed similarly abnormal US Doppler FPs in the SSS or the cerebral veins at any time (Fig 5).

#### US Doppler Flow Measurements during Follow-up

Only in patient 5 could serial Doppler measurements be evaluated after discharge. In the other patients, no or only single

examinations were performed during follow-up. None of these examinations showed retrograde flow components in the SSS or the cortical veins. Finally, 21 examinations could be included in this analysis.

Patient 5 showed a highly pathologic, retrograde, arterialized FP in both the SSS and cortical veins at re-admission. This pathologic FP developed during the first hospital stay (Fig 6A and Online Supplemental Data). At discharge (at the age of 9 weeks) and re-admission (at the age of 14 weeks), the SSS showed an arterialized FP toward the frontal base. At re-admission, there was also retrograde arterialized flow in the cortical veins. Direction of flow in the SSS and the cortical veins remained unchanged even after further embolization. Severe occlusion of the venous outflow due to bilateral stenosis of sinu-jugular junctions was finally diagnosed by MR imaging and invasive angiography, followed by endovascular therapy with bilateral balloon dilation and additional stent implantation on the left side. With each dilation step, the Doppler US flow direction in the SSS and cortical veins became less arterialized until almost complete normalization at the end of the intervention (Fig 6B). The examination at re-admission due to status epilepticus at 9 months of age showed again an arterialized, retrograde flow in the SSS and cortical veins with a significant increase of cerebral damage due to venous congestion on cMRI (Online Supplemental Data). Restenosis of the sinu-jugular junction could be excluded. After >90% occlusion of the VGAM, complete normalization of the FP in the SSS was observed.

## DISCUSSION

This retrospective observational study evaluated the use of US Doppler FPs of the superficial cerebral sinus and veins to detect venous congestion in VGAM serving as a bedside, broadly available, and noninvasive method for serial assessment during therapy. Sufficient occlusion of the VGAM corresponded to normalization of US Doppler FPs. Vice versa, persistent pathologic flow correlated with cerebral damage as measured on cMRI.

Normal US Doppler flow patterns of the cerebral veins are characterized by a continuous flat or sometimes slightly undulating profile. In the cerebral sinus, amplitude fluctuations up to a triphasic forward flow are more common.<sup>21-23</sup> These fluctuations correspond to the cardiac action and respiratory movements.<sup>24</sup> Recent advances in US technology allow the assessment of small cortical and medullary veins and analysis of intravascular flow even at low venous flow velocities.<sup>25</sup>

In this study, infants with VGAM frequently showed pathologic spectral US Doppler waveforms in the SSS with retrograde flow components, preinterventionally correlating with disease severity measured by the BNES. The proportion of pathologic FPs in the SSS decreased after partial superselective embolization, likely due to effective shunt reduction with concomitant pressure reduction in the cerebral venous system.<sup>5</sup>

In 1 patient, retrograde arterialized flow in the SSS occurred before discharge. Retrospectively, the increasing flow reversal resembled a venous outflow occlusion caused by bilateral stenosis of the jugular bulb. Serial US examinations during the endovascular reopening demonstrated the resolution of the FP abnormalities in real-time. After 5 months, complete retrograde flow in the SSS as well as in the cortical veins reoccurred, accompanied by

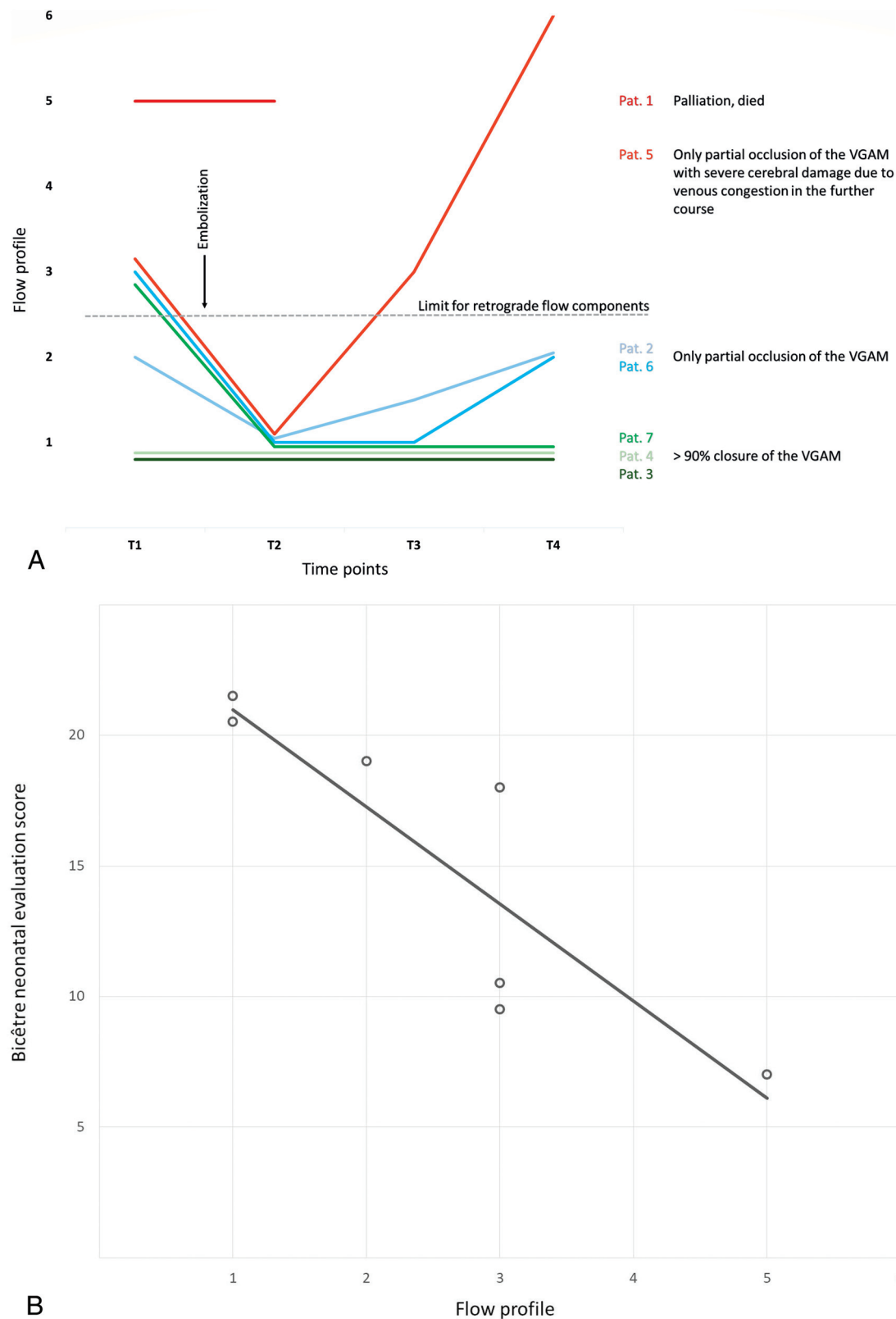


**FIG 4.** A, Individual course of the FPs in the SSS across time per patient. T1 = US Doppler measurement before embolization/first cMRI; T2 = US Doppler measurement 1 day after embolization/first cMRI; T3 = US Doppler measurement 5–7 days after embolization; T4 = US Doppler measurement before discharge. B, Association between Doppler FPs and BNES before therapy. Spearman rank correlation coefficient  $\rho = -0.97$  (95% CI,  $-0.995$  to  $-0.787$ ;  $P < .0001$ ). Pat. indicates patient.

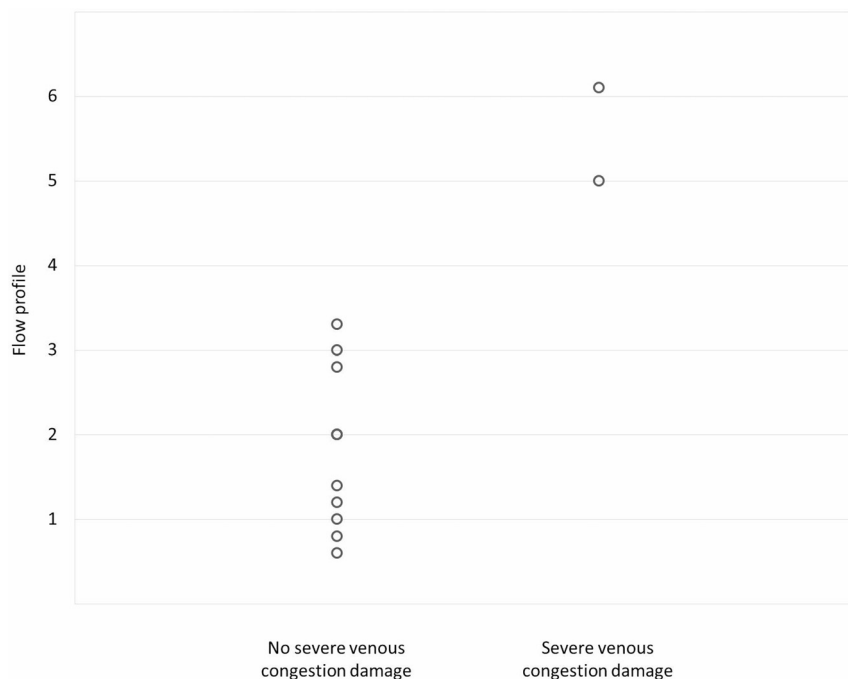


**FIG 5.** Relationship between the FP in the SSS at T1 and T4 and the damage due to venous congestion detectable in the first and second cMRI.

exacerbation of the cMRI findings. Consequently, almost complete embolization of the AV malformation resulted in a permanent normalization of the FPs.

A potential explanation for retrograde US Doppler flow components is the fluctuation of right atrial pressure during the cardiac cycle in patients with elevated central venous pressure. Tanaka et al<sup>26</sup> described pathologic FPs in the corresponding internal cerebral veins in 2 preterm infants with high-grade intraventricular hemorrhage. They attributed the retrograde flow components to increased venous pulsation caused by increased atrial contraction waves. The reverse flow corresponded to A and V waves, probably generated by an increase in right atrial pressure.<sup>26</sup> This may also play an important role in patients with VGAM with backward failure of the right heart. Another reason for insufficient venous outflow of the SSS in VGAM could be arterialized pressure in the confluence of sinuses or accessory confluence of sinuses. Quisling and Mickle<sup>6</sup> performed invasive venous pressure measurements within the Galen aneurysm/straight sinus complex in patients with Galen AVFs and vein of Galen aneurysms. The pressure was above the normal range (<5 cm H<sub>2</sub>O) in all cases and varied between 9 and 55 cm H<sub>2</sub>O. Values >20 cm H<sub>2</sub>O were associated with an increased incidence of cerebral calcifications as a typical sign of congestion damage. Venous outflow obstruction might be exacerbated by peak pressure during systole, possibly explaining the pulsatile reflux into the SSS sometimes observed.

Fluctuations in central venous pressure can be transmitted into the intracranial veins only in the absence of mechanical outflow obstruction. Probably, mechanical outflow obstruction initially leads to rising prestenotic pressure, increasing the pulsatile reflux into the SSS. Later, the complete or partial venous outflow from the AV malformation across the SSS directs the arterialized retrograde flow toward the frontal base. If the pressure in the SSS

exceeds the pressure in the afferent cortical veins, this scenario may result in a loss of normal ventriculocortical venous flow direction in the cortex and subcortical white matter. In the absence of sufficient collateral outflow tracts, this loss leads to venous congestion with subsequent parenchymal damage. Therefore, highly retrograde Doppler flow in the SSS is associated with pathologic FPs in the cortical veins and cerebral congestion damage on cMRI.

Real-time assessment of cerebral venous pressure is a diagnostic challenge. Accurate measurement can only be performed intracranially during angiography and is, therefore, not feasible as a routine diagnostic method for serial assessment. Currently, the only noninvasive tool to detect venous congestion is the appearance of indirect signs or direct parenchymal damage due to chronic venous congestion measured by cMRI.<sup>6,13-15</sup> Alterations on cMRI occur as late signs when damage has already occurred. In addition, cMRI scans cannot be repeated serially due to logistic and financial limitations and frequently require sedation or even anesthesia. Noninvasive methods for serial screening, monitoring, and follow-up of venous congestion would, therefore, be of great benefit for individual therapeutic management in VGAM.

Our study is limited by the sample size and retrospective design. This limitation is because VGAM is extremely rare, with approximately 1:58 100 live births per year in Germany.<sup>27</sup> The limited number of patients limits the possibility of conducting advanced statistical analyses. Furthermore, the criterion standard used to diagnose venous congestion in this study, namely cMRI, has a time lag between the onset of venous congestion and the manifestation of parenchymal damage detectable by this method.

Intracranial venous pressure is particularly influenced by central venous pressure, which, in turn, depends on volume status, cardiac function, and right ventricular and pulmonary artery

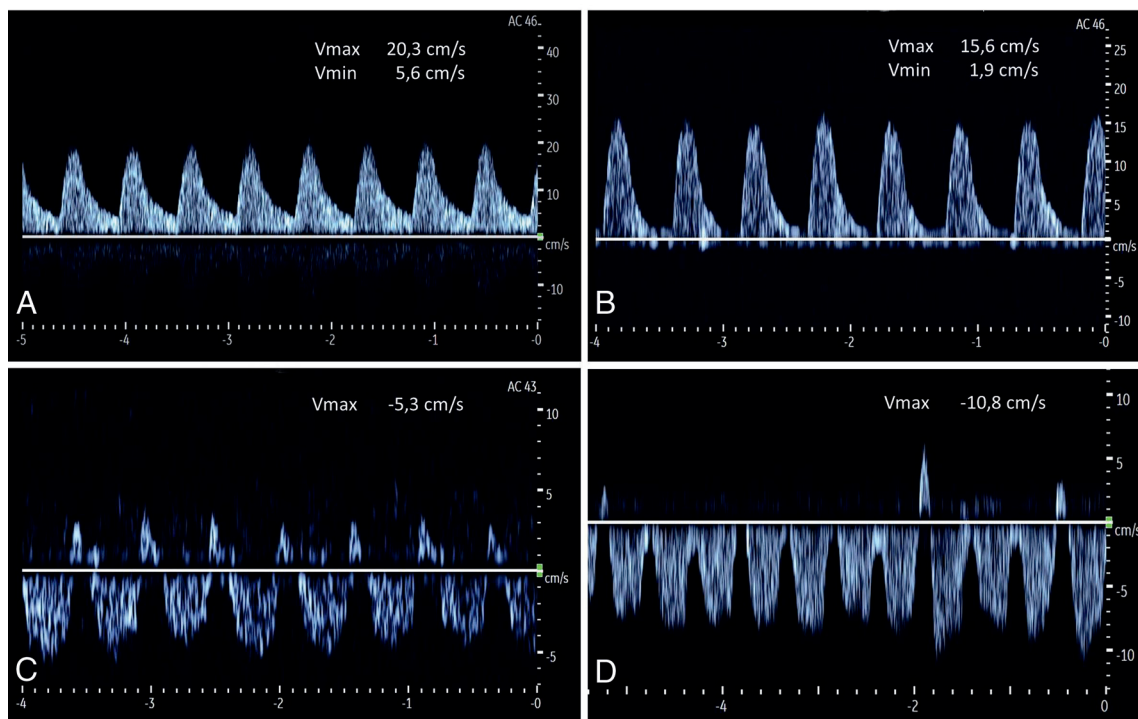
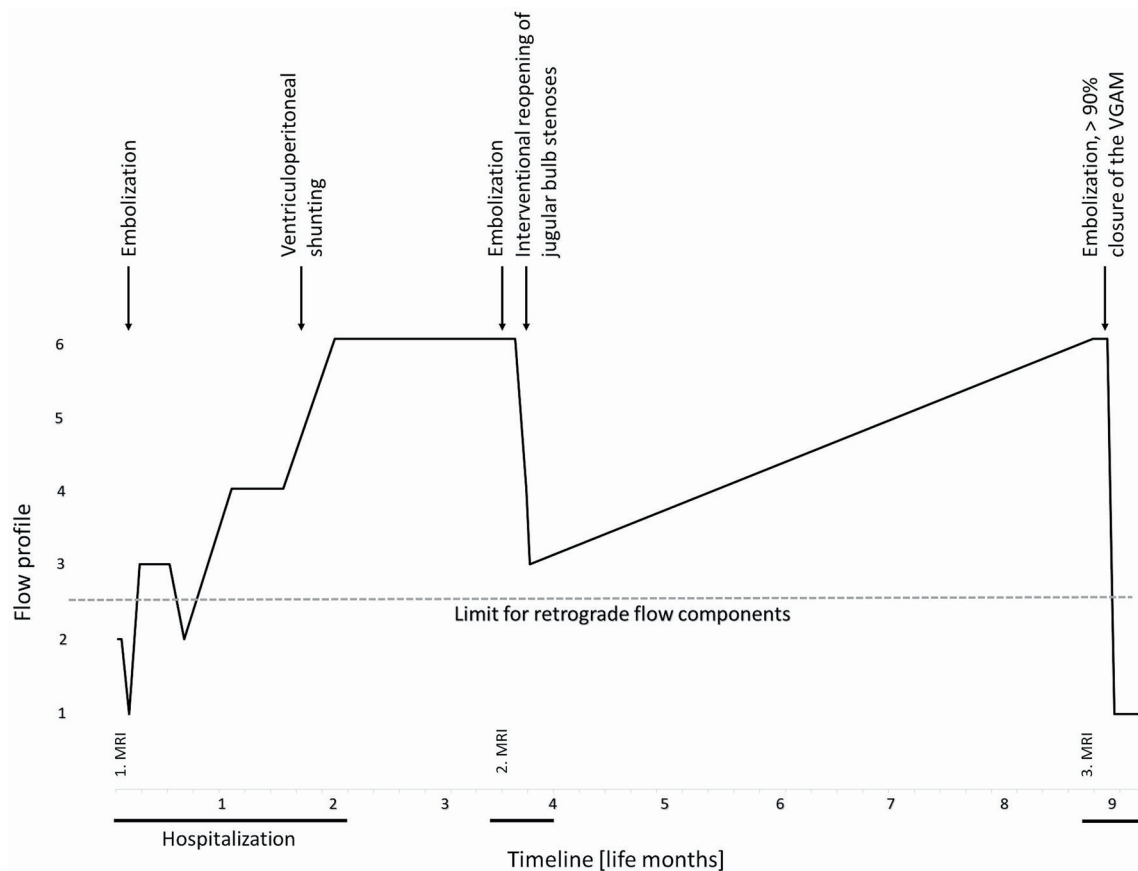


**FIG 6.** A, Timeline of the FPs in the SSS during 9 life months in patient 5. B, Course of Doppler FPs in the SSS under endovascular interventional therapy of stenosis of the jugular bulb in patient 5 (in the angiography room at the age of 16 weeks). A (upper left), An US Doppler FP in the SSS directly before balloon dilation on the left showing an arterialized retrograde flow. B (upper right), After balloon dilation and stent implantation on the left side decrease in flow velocities with reduced retrograde flow. C (bottom left), After additional balloon dilation on the right side, further reduction of the retrograde flow component and normalization of the flow direction. D (bottom right), At 24 hours after the procedure, further normalization of the US Doppler FP and increased undulation with minor retrograde components. Vmax indicates maximum velocity; Vmin, minimum velocity.



pressures. Therefore, both central venous pressure and cerebral venous US Doppler FPs may be affected not only by embolization itself but also by supportive measures or changes of the cardiocirculatory status. These include drug therapies (preload-lowering agents, inotropes, vasodilators, and sedation) and changes in circulatory conditions due to spontaneous closure or reopening of the ductus arteriosus (including prostaglandin E1 therapy) and must indispensably be considered when interpreting serial measurements.

Direct sonographic determination of the actual venous pressure is impossible. In VGAM, Doppler US in the SSS and cortical veins allows only a semiquantitative assessment of current hemodynamics caused by obstructed outflow of the superficial veins and thus an indirect estimate of venous congestion in the cerebral cortex. The outflow from the deep cerebral veins, which are directly affected by the increase in pressure in the persistent MPV, cannot be estimated with this method. Venous congestion leads to the formation of various venous collaterals. The veins involved in the collateral circuits exhibit sectional retrograde flow and may persist even after complete closure of all AV shunts of the VGAM, contributing to physiologic drainage of the brain parenchyma.

Yet, in patients with VGAM, US Doppler flow measurements of the superficial cerebral sinus and veins appear to have great potential to improve patient care and possibly neurologic outcome by providing the possibility of noninvasively monitoring cerebral venous hemodynamics in real-time. The data presented suggest that it is reasonable to integrate the US assessment of venous cerebral outflow in patients with VGAM into routine care. Further prospective studies should investigate the relevance of cerebral venous Doppler measurements for intensive care and endovascular therapy management in these neonates and in the prenatal diagnostics of fetuses with VGAM.

Besides this specific patient group, our study also points to the general potential of cerebral venous US Doppler flow measurements toward an understanding of cerebral venous hemodynamics in neonates. Abnormalities of venous US Doppler FPs cannot be expected only in VGAM but also in other diseases with cerebral venous outflow or upper cardiac inflow congestion. With ongoing technical advancements,<sup>28</sup> the cerebral venous system deserves increased attention both scientifically and in clinical practice to evaluate the clinical relevance of different venous Doppler waveforms in neonates with complex hemodynamic conditions.

## CONCLUSIONS

Flow reversal in the SSS measured with spectral Doppler US is a promising new diagnostic parameter for the assessment of venous congestion in VGAM. Relevant retrograde flow may indicate cerebral venous outflow obstruction due to increased central or cerebral venous pressure or mechanical occlusions and should prompt further diagnostic measures. As US techniques evolve, the potential of cerebral venous Doppler waveforms should be more systematically explored.

## ACKNOWLEDGMENTS

The authors would like to thank Mr Yannick Schulz for graphic assistance.

**Disclosure forms** provided by the authors are available with the full text and PDF of this article at [www.ajnr.org](http://www.ajnr.org).

## REFERENCES

1. Raybaud CA, Strother CM, Hald JK. **Aneurysms of the vein of Galen: embryonic considerations and anatomical features relating to the pathogenesis of the malformation.** *Neuroradiology* 1989;31:109–28 [CrossRef Medline](#)
2. Taffin H, Maurey H, Ozanne A, et al. **Long-term outcome of vein of Galen malformation.** *Dev Med Child Neurol* 2020;62:729–34 [CrossRef Medline](#)
3. Lecce F, Robertson F, Rennie A, et al. **Cross-sectional study of a United Kingdom cohort of neonatal vein of Galen malformation.** *Ann Neurol* 2018;84:547–55 [CrossRef Medline](#)
4. Chow ML, Cooke DL, Fullerton HJ, et al. **Radiological and clinical features of vein of Galen malformations.** *J Neurointerv Surg* 2015;7:443–48 [CrossRef Medline](#)
5. Chang D, Babadjouni R, Nisson P, et al. **Transvenous pressure monitoring guides endovascular treatment of vein of Galen malformation: a technical note.** *Pediatr Neurosurg* 2021;56:401–06 [CrossRef Medline](#)
6. Quisling RG, Mickle JP. **Venous pressure measurements in vein of Galen aneurysms.** *AJNR Am J Neuroradiol* 1989;10:411–17 [CrossRef Medline](#)
7. Kortman H, Navaei E, Raybaud CA, et al. **Deep venous communication in vein of Galen malformations: incidence, imaging, and implications for treatment.** *J Neurointerv Surg* 2021;13:290–93 [CrossRef Medline](#)
8. Meila D, Grieb D, Melber K, et al. **Hydrocephalus in vein of Galen malformation: etiologies and therapeutic management implications.** *Acta Neurochir (Wien)* 2016;158:1279–84 [CrossRef Medline](#)
9. Cory MJ, Durand P, Sillero R, et al. **Vein of Galen aneurysmal malformation: rationalizing medical management of neonatal heart failure.** *Pediatr Res* 2023;93:39–48 [CrossRef Medline](#)
10. Saliou G, Dirks P, Sacho RH, et al. **Decreased superior sagittal sinus diameter and jugular bulb narrowing are associated with poor clinical outcome in vein of Galen arteriovenous malformation.** *AJNR Am J Neuroradiol* 2016;37:1354–58 [CrossRef Medline](#)
11. Brew S, Taylor W, Reddington A. **Stenting of a venous stenosis in vein of Galen aneurysmal malformation: a case report.** *Interv Neuroradiol* 2001;7:237–40 [CrossRef Medline](#)
12. Gupta G, Rallo MS, Goldrich DY, et al. **Management of jugular bulb stenosis in pediatric vein of Galen malformation: a novel management paradigm.** *Pediatr Neurosurg* 2021;56:584–90 [CrossRef Medline](#)
13. Alvarez H, Garcia Monaco R, Rodesch G, et al. **Vein of Galen aneurysmal malformations.** *Neuroimaging Clin N Am* 2007;17:189–206 [CrossRef Medline](#)
14. Issa R, Barakat A, Salman R, et al. **Vein of Galen malformation, a cause of intracranial calcification: case report and review of literature.** *J Radiol Case Rep* 2019;13:13–18 [CrossRef Medline](#)
15. El Mekabaty A, Pearl MS, Merishon B, et al. **Susceptibility weighted imaging in infants with staged embolization of vein of Galen aneurysmal malformations.** *J Neuroradiol* 2019;46:214–21 [CrossRef Medline](#)
16. Lasjaunias PL. *Vascular Diseases in Neonates, Infants and Children: Interventional Neuroradiology Management.* Springer-Verlag; 1997
17. Lasjaunias PL, Chng SM, Sachet M, et al. **The management of vein of Galen aneurysmal malformations.** *Neurosurgery* 2006;59:S184–94; discussion S3–13 [CrossRef Medline](#)
18. Ikeda T, Amizuka T, Ito Y, et al. **Changes in the perfusion waveform of the internal cerebral vein and intraventricular hemorrhage in the acute management of extremely low-birth-weight infants.** *Eur J Pediatr* 2015;174:331–38 [CrossRef Medline](#)
19. Woodward LJ, Anderson PJ, Austin NC, et al. **Neonatal MRI to predict neurodevelopmental outcomes in preterm infants.** *N Engl J Med* 2006;355:685–94 [CrossRef Medline](#)
20. Meila D, Hannak R, Feldkamp A, et al. **Vein of Galen aneurysmal malformation: combined transvenous and transarterial method using a “kissing microcatheter technique.”** *Neuroradiology* 2012;54:51–59 [CrossRef Medline](#)

21. Dean LM, Taylor GA. **The intracranial venous system in infants: normal and abnormal findings on duplex and color Doppler sonography.** *AJR Am J Roentgenol* 1995;164:151–56 [CrossRef Medline](#)
22. Liu LY, Hong JL, Wu CJ. **A preliminary study of neonatal cranial venous system by color Doppler.** *Biomed Res Int* 2019;2019:7569479 [CrossRef Medline](#)
23. Taylor GA. **Intracranial venous system in the newborn: evaluation of normal anatomy and flow characteristics with color Doppler US.** *Radiology* 1992;183:449–52 [CrossRef Medline](#)
24. Deeg KH. **Duplex sonographic diagnosis of perinatal hemorrhagic stroke.** *Ultraschall Med* 2017;38:484–98 [CrossRef Medline](#)
25. Parodi A, Govaert P, Horsch S, et al; eurUS.brain group. **Cranial ultrasound findings in preterm germinal matrix haemorrhage, sequelae and outcome.** *Pediatr Res* 2020;87:13–24 [CrossRef Medline](#)
26. Tanaka K, Sakamoto R, Imamura H, et al. **Reversal of blood flow in deep cerebral vein in preterm intraventricular hemorrhage: two case reports.** *BMC Pediatr* 2020;20:517 [CrossRef Medline](#)
27. Brevis Nunez F, Dohna-Schwake C. **Epidemiology, diagnostics, and management of vein of Galen malformation.** *Pediatr Neurol* 2021;119:50–55 [CrossRef Medline](#)
28. Baranger J, Demene C, Frerot A, et al. **Bedside functional monitoring of the dynamic brain connectivity in human neonates.** *Nat Commun* 2021;12:1080 [CrossRef Medline](#)